

ORIGINAL PAPER

T. M. Weatherby · A. D. Davis
D. K. Hartline · P. H. Lenz

The need for speed. II. Myelin in calanoid copepods

Accepted: 8 January 2000

Abstract Speed of nerve impulse conduction is greatly increased by myelin, a multi-layered membranous sheath surrounding axons. Myelinated axons are ubiquitous among the vertebrates, but relatively rare among invertebrates. Electron microscopy of calanoid copepods using rapid cryofixation techniques revealed the widespread presence of myelinated axons. Myelin sheaths of up to 60 layers were found around both sensory and motor axons of the first antenna and interneurons of the ventral nerve cord. Except at nodes, individual lamellae appeared to be continuous and circular, without seams, as opposed to the spiral structure of vertebrate and annelid myelin. The highly organized myelin was characterized by the complete exclusion of cytoplasm from the intracellular spaces of the cell generating it. In regions of compaction, extracytoplasmic space was also eliminated. Focal or fenestration nodes, rather than circumferential ones, were locally common. Myelin lamellae terminated in stepwise fashion at these nodes, appearing to fuse with the axolemma or adjacent myelin lamellae. As with vertebrate myelin, copepod sheaths are designed to minimize both resistive and capacitive current flow through the internodal membrane, greatly speeding nerve impulse conduction. Copepod myelin differs from that of any other group described, while sharing features of every group.

Key words Crustacean · Sensorimotor · Ultrastructure · Multilamellar sheath · Myelinated axons

T. M. Weatherby
Biological Electron Microscope Facility,
Pacific Biomedical Research Center,
University of Hawaii at Manoa,
1993 East-West Rd., Honolulu, HI 96822, USA

A. D. Davis · D. K. Hartline · P. H. Lenz (✉)
Békésy Laboratory of Neurobiology, Pacific Biomedical Research
Center, University of Hawaii at Manoa, 1993 East-West Rd.,
Honolulu, HI 96822, USA
e-mail: petra@pbrc.hawaii.edu
Fax: +1-808-956-6984

Introduction

Myelin is one of the key innovations promoting the success of the vertebrates. Without it, rapid reactions to external stimuli and fast, compact brains would be difficult to engineer. Myelination confers an order of magnitude gain in the speed of nerve impulse propagation compared to unmyelinated nerve, as well as great savings in energy and space. It is thus perhaps surprising that, while not unknown among invertebrates, it is uncommon. Myelin-like wrapping of nerve fibers and the presence of nodes have been described at the electron microscope level in annelids (e.g., Günther 1976; Roots and Lane 1983) and malacostracan crustaceans (palaemonid shrimp: Heuser and Doggenweiler 1966; penaeid shrimp: Kusano 1966; Xu and Terakawa 1999; alpheid shrimp: Govind and Pearce 1988). Recently, we reported the occurrence of myelin in three superfamilies of copepods (Davis et al. 1999; Lenz et al. 2000). In the present study, we characterize the structure of myelin in relation to its presumed function in calanoid nerve fibers. The sheaths of the copepods are highly organized and resemble myelination in several other groups, including vertebrates. They appear to differ significantly from those of most other groups in their mechanisms for preventing current shunting at potential weak points in the investment.

Materials and methods

Collection

The study focused on seven calanoid copepod species: *Gaussia princeps* (Augaptiloidea: Augaptilidae), *Candacia aethiopica* (Centropagoidea: Candaciidae), *Labidocera madurae* (Centropagoidea: Pontellidae), *Epilabidocera longipedata* (Centropagoidea: Pontellidae), *Undinula vulgaris* (Megacalanoidea: Calanidae), *Neocalanus gracilis* (Megacalanoidea: Calanidae), and *Euchaeta rimana* (Clausocalanoidea: Euchaetidae). These calanoids were collected as described in Lenz et al. (2000). Except for *E. longipedata*, all species were collected around the Hawaiian Islands: Kaneohe Bay, Oahu (*L. madurae*, *U. vulgaris*), 2–4 km offshore from Kaneohe Bay or Keauhou Bay, Kailua-Kona, Hawaii (*C. aethiopica*, *E. rimana*,

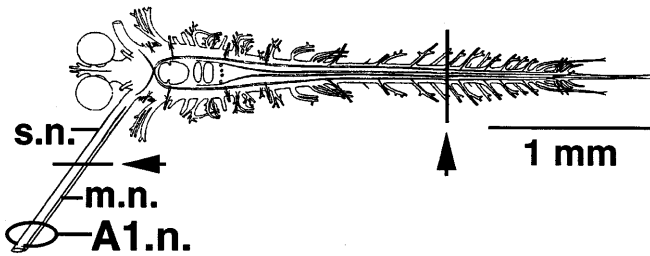


Fig. 1 Diagram of the nervous system of a calanoid copepod (*Epilabidocera amphitrites*), showing important features and locations of cross-sections obtained for electron microscopic analysis (arrows). Two pairs of giant fibers are depicted within the profile of the nervous system. *A1.n.* antennular nerve; *m.n.* antennular motor nerve; *s.n.* antennular sensory nerve. Modified from Park (1966)

N. gracilis) and 586 m deep pipe off Ke'ahole Point, Kailua-Kona, Hawaii (*G. princeps*). *E. longipedata* were collected off the dock at Friday Harbor Laboratories, Washington.

Transmission electron microscopy

Two different types of fixation methods for transmission electron microscopy (TEM) were utilized: chemical fixation and ultrarapid cryofixation. Prior to fixation, specimens were usually sedated with $MgCl_2$. For chemical fixation of the first antenna (A1 or antennule), penetration of fixative was improved by removing the A1 from the copepod, by making an incision directly into the antenna, or by removing individual setae. Access of fixative to the CNS was facilitated by making a cut in the urosome. Our conventional chemical fixation method using 4% glutaraldehyde and $0.1 \text{ mol} \cdot \text{l}^{-1}$ sodium cacodylate buffer with $0.35 \text{ mol} \cdot \text{l}^{-1}$ sucrose has been described in Weatherby (1981) and Weatherby et al. (1994). For ultrarapid cryofixation, the sedated copepods were blotted with tissue paper then plunged into freezing propane (-187°C) with a Reichert-Jung KF80 immersion cryofixation system. The specimens were transferred to a substitution medium consisting of 1% osmium tetroxide in either acetone or methanol at -190°C , then placed in a freezer (-80°C). After 6 days they were moved to another freezer (-20°C) for 24 h, then allowed to warm to room temperature, during which time the substitution medium was changed twice. After the copepods reached room temperature within ca. 5 h, they were infiltrated through propylene oxide to LX 112 (Ladd) epoxy resin and polymerized at 60°C . Ultrathin (80–90 nm) sections (Reichert Ultracut E ultramicrotome) through the first antenna concentrating on segment V (nomenclature follows Huys and Boxshall 1991) provided an easily identified and standard location with a large axonal population for all species. Sections of the ventral nerve cord were made at the level of the 1st and 2nd pereopods ("P1" and "P2"; Fig. 1, transverse line). Sections were double-stained with uranyl acetate and lead citrate, and viewed and photographed in a Zeiss 10/A and a LEO 912 EFTEM at 80 kV and 100 kV.

Results

Myelin and the gross morphology of copepod nerve

We first compared the gross morphology of myelinated and non-myelinated calanoid groups in regions of the nervous system related to escape behavior. In both groups, the paired first antennae ("A1" or antennules) provide the primary sensory input mediating hydrodynamically triggered escape (Gill 1985, 1986). Mechano-sensory axons, typically two per seta, originate from

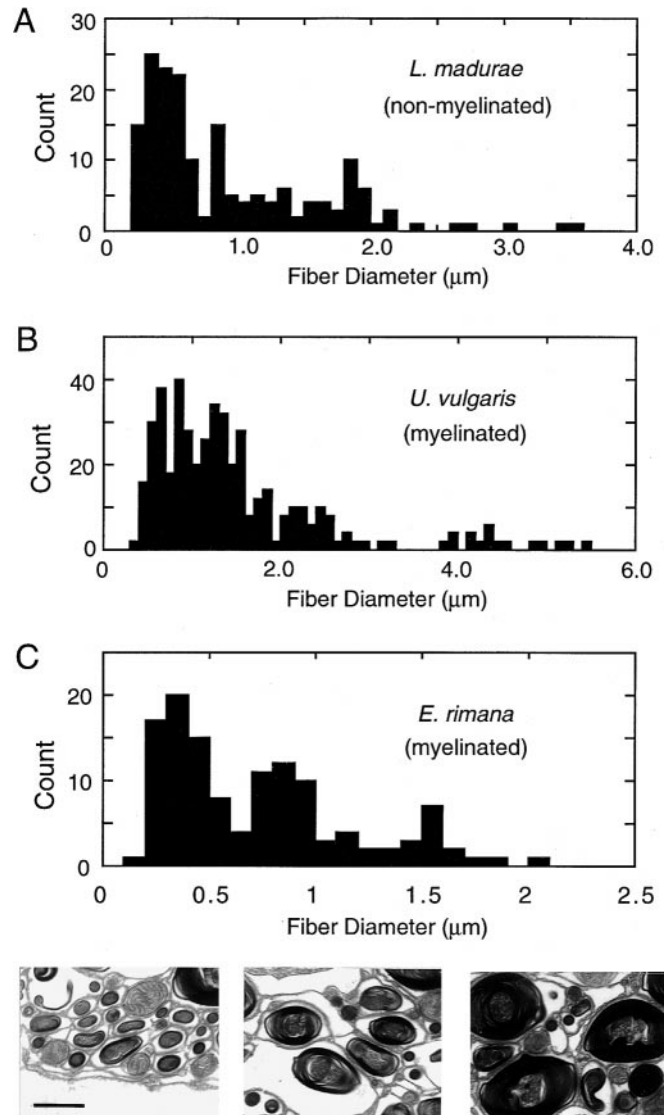


Fig. 2A–C Histograms of fiber diameters from the A1 sensory nerve of three representative copepods. Profiles of the outer perimeter of a nerve fiber and of the innermost circle of myelin were traced from EM images using NIH Image software (written by Wayne Rasband). Perimeters were converted to equivalent diameters by dividing by π . Histogram bins $0.1 \mu\text{m}$ wide. **A** *Labidocera madurae* (chemical fix). **B** *Undinula vulgaris* (cryofix). **C** *Euchaeta rimana* (cryofix). Note axon classes are half the diameters of those of *U. vulgaris*. Electron micrographs below show representative regions of nerve dominated by axons of the three size classes above. Bar = $1 \mu\text{m}$

spinose or plumose "T1" setae, most of which are located along the anterior margin of the A1. The other known sensory innervation gives rise to chemosensory axons from bimodal T1 setae (Lenz et al. 1996) and from "C1" aesthetascs (Bundy and Paffenhöfer 1993; Weatherby et al. 1994; Lenz et al. 1996). For any particular sex and life stage, the distribution pattern of these receptors is species-specific, so the axonal composition of the A1 sensory nerve (Fig. 1, *s.n.*) is expected to be relatively constant as well. In low-power electron-micrographic cross-sections of the nerve, in particular those

Table 1 Receptors and axons of first antenna. Table shows the species-specific setation pattern for three calanoid species and the expected contributions of the mechanoreceptors to axon counts made on one individual from each species at segment V. Calculations of expected mechanosensory fibers are based on two neurons per mechanosensory ("T1") seta (nomenclature of Fleming 1985), except for one (*Euchaeta rimana*) or two (*Undinula vulgaris* and *Labidocera madurae*) distal setae, which are singly innervated in *P. xiphias* (Weatherby et al. 1994; Lenz et al. 1996), and so are likely to be in other calanoids. Species-specific seta and aesthetasc numbers from SEM with light-microscope confirmation; numbers

are close to those published elsewhere for the species (*L. madurae*: Yen et al 1992; *U. vulgaris*: Fleming 1985). Counts commenced with segment VII, because axons of the sensory cells innervating setae and aesthetascs of more proximal segments join the nerve bundle proximal to segment V. Most mechanoreceptive axons can be accounted for by large and medium classes. Remaining axons, presumably chemoreceptive, correspond to the smaller-diameter fibers. Medium- and large-diameter fibers were defined as follows: *L. madurae*: >0.8 μm ; *U. vulgaris*: >1.6 μm ; *E. rimana*: >0.6 μm . These boundaries reflect discontinuities in the histograms (Fig. 2)

	<i>Labidocera madurae</i>	<i>Undinula vulgaris</i>	<i>Euchaeta rimana</i>
Whole antennule, segments I–XXVIII			
No. of T1 setae	53	57	48
No. of aesthetascs	18	24	8
Segment V cross-section			
No. of T1 setae; seg. VII–XXVIII	44	44	38
No. of aesthetascs; segs. VII–XXVIII	14	17	7
Expected no. of mechanosensory fibers	86	86	75
Total sensory fibers observed in specimen	175	248	124
Difference (= non-mechanosensory fibers)	89	162	49
No. of small-diameter fibers in specimen	97	179	61
Motor fibers	38	35	40

taken at segment V, axon size varied over a large range in all copepods examined, whether from myelinated or non-myelinated groups. This is illustrated in Fig. 2 with histograms of axon diameters for individuals of three species, one non-myelinated (*L. madurae*; Fig. 2A) and two myelinated (*U. vulgaris* and *E. rimana*, Figs. 2B and 2C, respectively). In all three, three size-classes are apparent. Approximately half of the axons form a small diameter class. The larger-diameter axons are presumably from mechanoreceptors. Their numbers approximate those expected from counts of T1 setae, as tabulated in Table 1. In *L. madurae*, two of the axons are particularly large (3.5 μm), possibly corresponding to the A and B units of the giant antennal mechanoreceptors identified electrophysiologically (Hartline et al. 1996). However, while none of the *E. rimana* axons were as large, some of the axons of *U. vulgaris* were even larger than those in *L. madurae*, so there was no clear difference in axon diameter between the myelinated and non-myelinated species. There are fewer small sized fibers in the *E. rimana* specimen, which is consistent with the smaller number of chemosensory setae (aesthetascs) in this species (Table 1). In *U. vulgaris* and *E. rimana* nearly all axons in the A1 sensory nerve at segment V (Fig. 2C; see also Lenz et al. 2000), were myelinated. Occasionally, unmyelinated profiles were observed, but it was not clear that these were axons. As there are more myelinated fibers than needed to account for known mechanoreceptors, we conclude that A1 chemosensory axons are myelinated as well.

The central component of the escape response involves paired giant interneurons connected to segmental motor neurons (Lowe 1935; Park 1966; see diagram in Fig. 1). Both non-myelinated and myelinated species possessed giant axons in the ventral cord (Figs. 3C, 5C). In the myelinated species, a substantial (but unquantified)

fraction of axons in the nerve cord was myelinated at the P1-P2 level (Fig. 3C). The bilateral pairing of the larger axons, heavily invested in myelin, was quite apparent in cross-section (Fig. 3C, upper-case letter pairs).

In addition to innervating swimming leg muscles, motor output innervates muscles present throughout the A1's (Boxshall 1985, 1992), allowing A1's to fold along the streamlined body during an escape response. For the animals presented in Table 1, A1 motor nerves in the cross-sections of myelinated species (Fig. 1, *m.n.*) had axon numbers similar to that for *L. madurae*. In *U. vulgaris* and *E. rimana* all motor axons in the A1 at segment V were myelinated (Fig. 3A). There is little evidence of any major differences in A1 innervation between non-myelinated and myelinated copepods.

In myelinated fibers, the thickness of the sheath varied, ranging from just 1 or 2 lamellae to over 50. The thickest sheaths observed in copepod A1 nerve still had fewer lamellae than the maximum reported in some vertebrate fibers. An important parameter in assessing efficiency of impulse conduction in vertebrate myelinated nerve is the ratio of the axon core diameter to the total fiber diameter (core plus sheath). Calculations suggest that a ratio of 0.62 yields the fastest conduction for a given total diameter (Moore et al. 1978). Figure 4 shows a scatter plot of this ratio for one A1 segment V of an *U. vulgaris*. Mean ratios were 0.61 ± 0.20 and 0.65 ± 0.23 for motor and sensory nerves, respectively. Although the mean is close to the vertebrate optimum, the scatter was substantially greater than for mouse vagus and sciatic nerve (Friede and Samorajski 1967). A ratio of 1, calculated for some of the smaller axons, was due to wraps of one or two layers, where the thickness of the sheaths was less than 30 nm. About half of the class of small axons in the figure have this minimal wrapping.

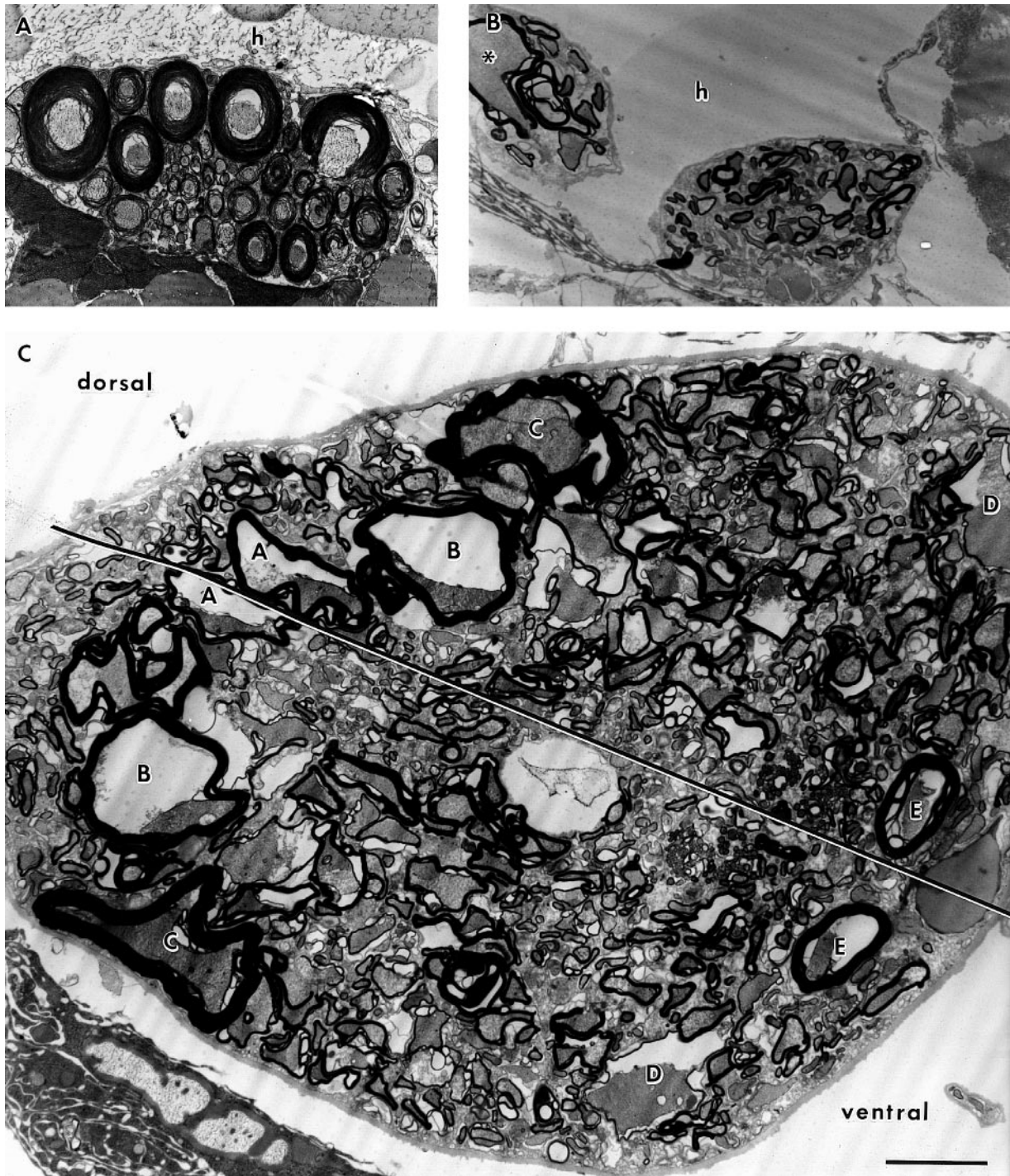


Fig. 3A–C Sections through the nervous system of cryofixed *U. vulgaris* showing the extent of myelination. **A** Motor nerve at segment V. **B** Section through thoracic motor nerves near the base of the second pereopod. Note giant motor axon (*). **C** Central nervous system near the base of the second pereopod. Profiles of heavily-myelinated axons show pair-wise correspondence (*A*, *B*, ... *E*) across the midline (*solid line*). *h* hemolymph sinus. Bar = 5 μ m

Myelinated versus unmyelinated nerve fibers

The fine structure of nerves of several non-myelinated copepods was examined to provide a frame of reference

for the studies of myelination. Similar to other crustacean nerves, unmyelinated axons of both the A1 (Fig. 5A,B) and the ventral nerve cord (Fig. 5C) were characterized by an abundance of microtubules distributed throughout an electron-lucent axoplasm. Mitochondria were small (0.3–0.5 μ m) but numerous, usually distributed peripherally, close to the axolemma. Abundances varied substantially, with some tracts of axons possessing significantly greater numbers (Fig. 5B) than others nearby. Axons in the interior of nerves were usually in close apposition to either other axons or to

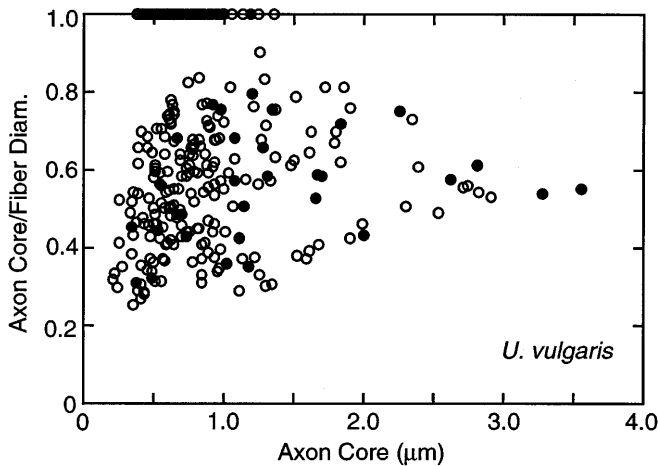


Fig. 4 Scatter plot of the ratio of axonal core to fiber diameter versus axonal core diameters for a single *U. vulgaris* from cryofixed material. *Open circles*: sensory nerve; *solid circles*: motor nerve

glial cells. The latter also possessed microtubules, an electron-lucent cytoplasm and small mitochondria. The primary feature that distinguished glia from axons was their possessing a thin, angular and sometimes sinuous profile interposed between the more rounded axonal profiles (Fig. 5). Very little, if any, of the multiple-wrapped glial and connective tissue sheathing typical of some crustacean nerve was found in the A1 nerves and ventral nerve cord at the base of the P2.

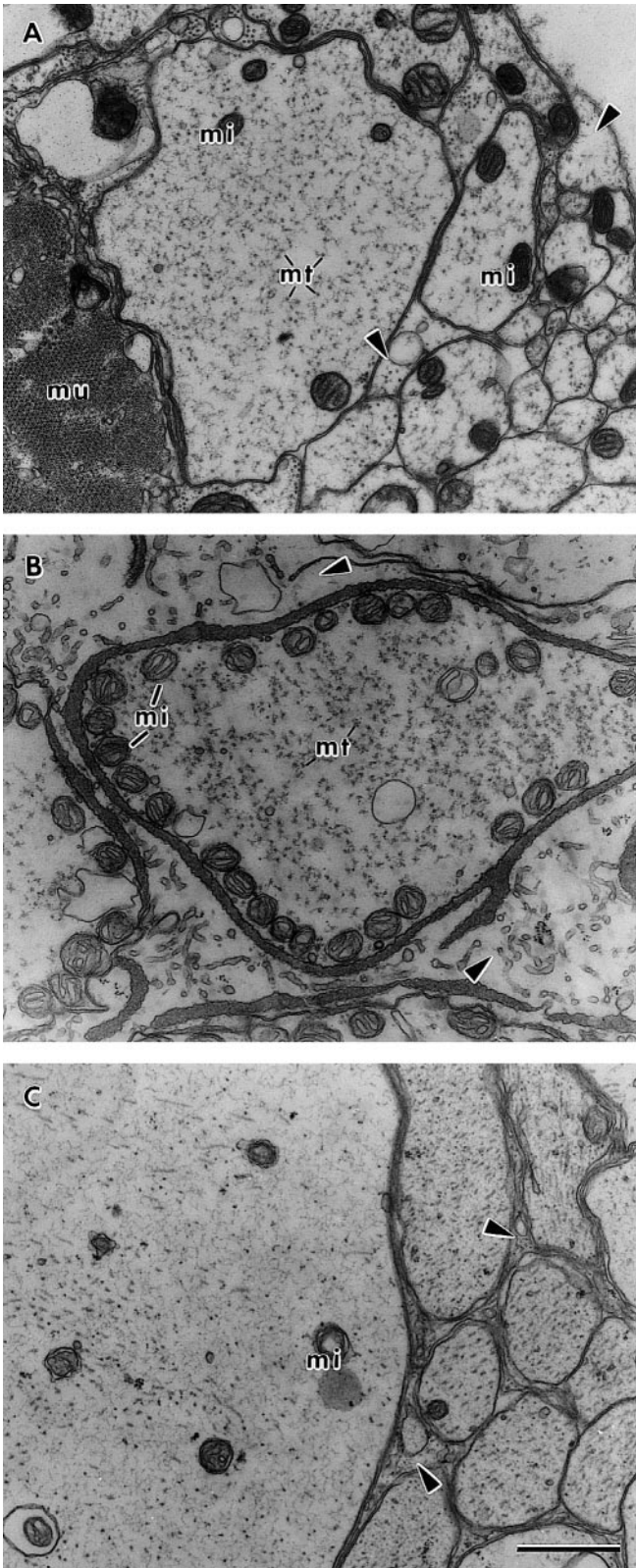
Features found in myelinated axons of the A1 are shown for two myelinated species, *N. gracilis* and *E. rimana* (Fig. 6A and B, respectively). These can be compared with those from two species lacking myelination, *C. aethiopica* and *G. princeps* (Fig. 5A and B). As in the case of unmyelinated axons, myelinated ones were characterized by an electron-lucent cytoplasm with an abundance of microtubules. Many fewer mitochondria were observed inside, consistent with lower metabolic requirements for myelinated axons. In addition to the myelin sheaths, the fibers were enveloped by glial cell processes which often contained short rows of microtubules (Fig. 6C, *mt*). Glial material between adjacent fibers or clusters of small fibers partitioned the nerve into compartments with substantial extracellular space between the glia and the outer myelin wrap in some places. In *E. rimana* especially, the glial partitions were very thin, with occasional small “beads” of cytoplasm along their length. No mesaxons were observed connecting glial cells with the myelin sheath of the enclosed nerve fibers. The axons were suspended in the extracellular space, without obvious contacts, even in material that appeared to be well fixed (Fig. 6C, *sp*). This was a marked contrast to unmyelinated nerve, in which there was very little extracellular space. Myelinated copepod nerves, whether peripheral (A1) or central, contained few glial cell bodies and nuclei within the trunks. Most were located along the edges of the nerve bundles, as in the non-myelinated species.

Organization of myelin sheaths

The myelin sheaths were studied in more detail in three calanoid species: *U. vulgaris*, *N. gracilis* and *E. rimana*. The sheaths of *U. vulgaris* and *N. gracilis* differed somewhat from that of *E. rimana* (cf. Fig. 6A, B). In small fibers with few layers in all three species, individual lamellae could be followed in a complete circle around the axon, showing a concentric organization (Fig. 7A), as opposed to the spiral organization of vertebrate myelin. From Fig. 7B it is clear that the axolemma (arrow) is separated from the first thick myelin wrap (arrowhead) by an electron-lucent space. Although this space appears to be extracytoplasmic—devoid of cytoplasmic material—we could not confirm whether it was extracellular. The repeating pattern for successive rings (noticeably thicker owing to fusion of two membranes: see below) indicates that the clear laminae represent extracytoplasmic space. The concentric layers appeared uniform with no evidence of “seams” or “cytoplasmic loops” such as those described in the myelin sheaths of prawn (Heuser and Doggenweiler 1966) or penaeid shrimp (Xu and Terakawa 1999). It was not possible to determine the wrapping pattern in many of the sheaths, either because the laminae were distorted and layers became confused, or because (especially in *E. rimana*) sheaths contained extensive condensed areas in which laminar substructure could not be discerned (Fig. 7B, C, *cz*).

Myelin laminae were tightly wrapped around a microtubule-filled axon. Laminae consisted of osmiophilic layers alternating with the electron-lucent extracytoplasmic layers, which were of more variable thickness (Fig. 7B). The dark layers appeared to represent the fusion of the intracellular surfaces of the sheath-cell membrane, devoid of intervening cytoplasm. The axolemma was a typical single “unit” membrane of 9 nm thickness (Fig. 7B, arrow). The myelin sheath laminae were 18 nm in thickness, consistent with their being two fused membranes. In favorable regions, a trilaminar aspect could be discerned with a central, particularly electron dense line (major dense line) flanked by lower density regions. The outermost sheath layer was 35–40 nm thick, consistent with its appearance as two fused laminae, or four unit-membranes total (Fig. 7C, arrow). The electron-lucent extracytoplasmic layers ranged in thickness from 30 nm to 3 nm between the outermost layers, with the space often decreasing with distance from the central axon. An extracytoplasmic space ranging from 10 nm to 40 nm separated the axoplasmic membrane from the innermost layer of the myelin sheath (10–20 nm is typical for both prawn and vertebrate; e.g., Heuser and Doggenweiler 1966).

The myelin sheaths in *E. rimana* had extensive areas where the extracytoplasmic space virtually disappeared. In these condensation zones, the sheath decreased in width and assumed a dark gray finely granular appearance showing little substructure (Fig. 7B, C, *cz*). When present, the condensation zones distorted the otherwise circular fiber profile. Because of this close spacing there



◀
Fig. 5A–C Transmission electron micrographs (TEMs) of axonal cross-sections from nerves of non-myelinated copepods. **A** A1 (first antenna) nerve from *Candacia aethiopica* showing the largest axon at segment V (cryofix). **B** Mitochondria-filled axon from motor nerve (A1) from *Gaussia princeps* (chemical fix). **C** Ventral nerve cord from *Epilabidocera longipedata* showing part of the medial giant axon on the left, as well as smaller axons (chemical fix). *mi* mitochondria; *mt* microtubules; *mu* muscle. Arrowheads indicate glial processes. Bar = 1 μ m

Doggenweiler 1966). Areas of condensation were also observed in the megacalanoideans, but not with the consistency or the extent seen in *E. rimana*.

A few large cells containing nuclei were observed enclosed within a myelin sheath (Fig. 7D), similar to the descriptions of sheath cells by Heuser and Doggenweiler (1966). Occasionally, a cell with a large nucleus was found outside of, but in apparent association with, a myelinated axon (not shown). However, in material examined to date, cell bodies associated with myelin have been found only along the anterior margin of the A1 in regions associated with the sensory dendrites of anteriorly-projecting setae. It has not been determined whether they are glial or neuronal.

Nodes

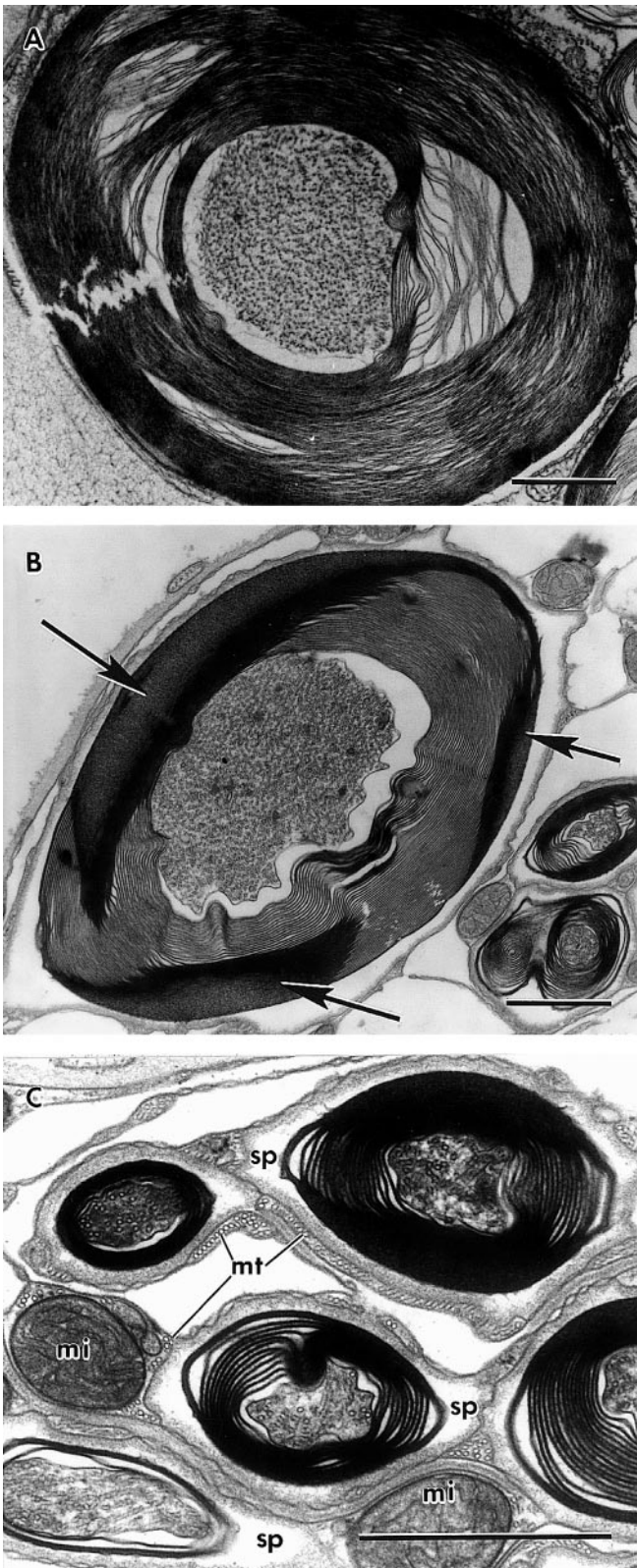
Discontinuities in the myelin sheaths of sensory and motor axons resembled “fenestration” or “focal” nodes as described for other invertebrates (Günther 1976; Hsu and Terakawa 1996). These nodes were found in *E. rimana* (Fig. 7E, F), *U. vulgaris* (Fig. 3A) and *N. gracilis*. At these nodes, individual laminae terminated in close step-wise order at the axolemma: the innermost layers terminated first and the outermost last. Thus, each layer ended in contact with either the axolemma or a density (Fig. 7E). So far, using TEM cross-sections, we have not been able to detect any nodes that wrap around the entire circumference of the axolemma. The exposed axolemma membrane was not in contact with any clear cellular membrane, but seemed to be exposed to the extracellular space, generally including a basal lamina surrounding the axon (Fig. 7E, *bl*). There was no evidence of nodal glial cells of the sort found in prawns (Heuser and Doggenweiler 1966). At neuromuscular synaptic sites, myelination extended right up to the synapses. The laminae terminated in the same fashion as in nodes, leaving the naked axolemma free at the neuromuscular gap. Presynaptic specializations and vesicles were seen (Fig. 7F).

Discussion

Myelin function

Myelin serves three potential functions: (1) to increase conduction velocity for nerve impulses; (2) to reduce space requirements for nerve fibers; and (3) to reduce metabolic costs. An increase in conduction velocity (by

did not appear to be room for any additional structures, such as desmosomes or other junctional sites. Overall the appearance of these zones was more similar to compacted vertebrate myelin than to the radial attachment zones described for the prawn (Heuser and



◀ **Fig. 6A–C** Comparison of motor axons from the first antenna in segment V from adult females of two species (cryofixed material). **A** *Neocalanus gracilis*. Individual axon ensheathed by multiple layers of myelin. In areas exhibiting freezing damage, myelin laminae appear to be separated with individual laminae appearing ruffled. **B** *E. rimana*, axons. The lamellae are closely and regularly spaced. *Arrows* point to condensation zones in which layering is difficult to discern. **C** *E. rimana* motor nerve showing periaxonal spaces (*sp*); thin glial partitions between axon compartments; glial microtubules (*mt*) and mitochondria (*mi*). Note compacted myelin of outermost laminae. Bar = 1 μm

common predator warning comes from mechanical signals (Gill 1985), explaining the myelination of mechanosensory, as well as motor and giant central fibers involved in escape responses. Explaining myelination of fibers subserving chemoreceptive modalities, which are intrinsically slow and would not be expected to profit much from faster axonal conduction, seems to require a different mechanism. With approximately 10–20% of the axonal volume of a sensory nerve being small-diameter fibers (presumed chemoreceptive), a metabolic saving (up to 10,000-fold; e.g., Bullock and Horridge 1965) might be of significance, especially for a copepod living in an oligotrophic (nutrient-poor) environment such as the open ocean.

In copepods, neither the presence of myelin nor its significance has been widely recognized (Davis et al. 1999). Early reports (Lowe 1935; Barrientos 1980) in *Calanus finmarchicus* have been overlooked in more recent literature. In the calanoids we have found highly organized multilamellar sheaths enveloping nerve fibers of the central and the peripheral (sensory and motor) nervous system. Myelination of sensory axons occurs in vertebrates, but has not been reported in the annelids and most malacostracans (Roots 1984). Govind and Pearce (1988), however, describe the occurrence of myelin in both sensory and motor axons of snapping shrimp (*Alpheus californiensis* and *A. heterochelis*). This is one of the few examples of extensive myelination of axons in peripheral nerves in the invertebrates and as such is similar to the copepod.

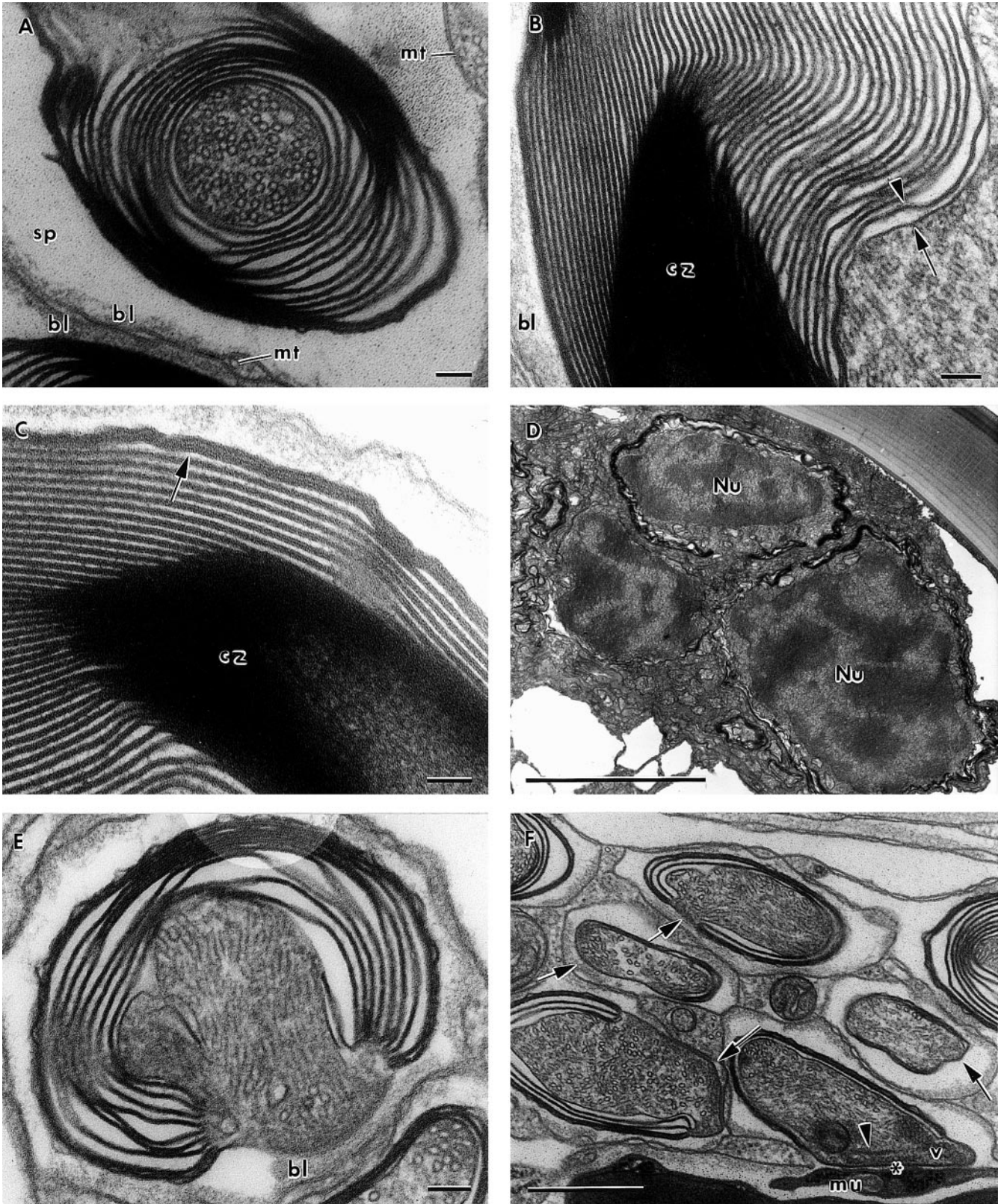
Copepod myelin has characteristics of both vertebrate and invertebrate myelin

In the invertebrates, myelin has been characterized by the lack of a single design. Our results add to the recorded diversity of invertebrate myelin. In the copepod, the myelin is highly organized resembling the well-organized wrapping found in the vertebrates (see Table 2).

Wrap topology

In vertebrates, myelin is formed by multiple layers of spirally wrapped glial cell membrane (for reviews, see Morell 1984; Zagoren and Fedoroff 1984). A spiral wrap is also typical of annelids (Roots and Lane 1983), but

an estimated factor of ten; Ritchie 1984) can help explain decreases in reaction times to predatory lunges observed in myelinated groups (Lenz et al. 2000). It may also enhance the reaction capabilities of a myelinated predator (such as *E. rimana*). For copepods, the most



among crustaceans, this arrangement is rare (review: Roots 1984). In the palaemonid and penaeid shrimp, sheaths are formed from concentric glial layers which encircle the fiber, forming “cytoplasmic loops” and

“seams” at the abutment of adjacent glial processes of the same layer. For copepods, where layers were distinct (e.g., Fig. 7A), the wraps were concentric and continuous, unlike either vertebrates or malacostracans.



Fig. 7A–F High magnifications of features of myelinated nerve in *E. rimana* (cryofixed). **A** Small axon showing microtubule-packed axoplasm and uninterrupted concentric myelin lamellae. Each periaxonal space (*sp*) is lined with basal lamina (*bl*). A thin glial cell process containing patches of microtubules (*mt*) and “beaded” with regions of thicker cytoplasm in places surrounds periaxonal space. **B** At high magnification, individual 18-nm-thick laminae are seen as two fused 9-nm membranes. Space between the single membrane axolemma (*arrow*) and the double thickness myelin lamina (*arrowhead*), as well as other electrolucent lines, is extracytoplasmic. Note condensation zone (*cz*). **C** At high magnification the outer layer is seen to be composed of two fused laminae (*arrow*). **D** Myelinated cell bodies (interrupted by nodes). Large nuclei (*nu*) surrounded by thin bands of cytoplasm. **E** At nodes myelin laminae terminate against axoplasm leaving the axolemma naked against the basal lamina (*bl*). **F** At neuromuscular synapses (*) myelin laminae end at the axolemma in the same pattern as at nodes, and presynaptic membranes are closely apposed to the muscle cells. Note nodes (*arrows*) in adjacent fibers. Adult female, first antenna, segment V, cryofixed. *mu* muscle, *v* vesicles, *bl* basal lamina, *arrowhead* presynaptic specializations. **A, B, C and E:** bars = 0.1 μm ; **D:** bar = 5 μm , **F:** bar = 0.5 μm

Compaction

In *E. rimana*, the electron-dense layers appeared to be composed of two membranes, fused along the intracellular leaflet, with no intervening cytoplasm. The dense line thus formed would correspond to the “major dense line” of vertebrate myelin. The absence of cytoplasm between layers is also typical of penaeid myelin (Xu and Terakawa 1999). In contrast to this situation, the myelin of prawns and annelids is characterized by the near absence of *extracellular* space, while thin ribbons of cytoplasm remain separating the intracellular faces (Heuser and Doggenweiler 1966; Roots and Lane 1983). Elimination or near elimination of the extracytoplasmic (as well as cytoplasmic) space was seen in the outer two wraps for each axon of *E. rimana* and may be present in the Megacalanoidea as well, albeit intraperiod lines were

not clearly discernible. The condensation zones may represent similar compaction. In prawns, annelids and penaeids, patches of desmosome-like “radial attachment zones” are present, at which membrane spacing increases and fills with electron-dense material (Heuser and Doggenweiler 1966; Roots and Lane 1983; Xu and Terakawa 1999). Comparable structures have not been seen in copepods.

Glial relationships

In both vertebrates and invertebrates, the myelin layers are formed by glial cells. In the vertebrates, the cell body of the glial cell forming the layers is typically located externally (Schwann cell or oligodendrocyte). In malacostracans and annelids, glial cytoplasm and nuclei are located inside the sheath (Heuser and Doggenweiler 1966; Roots and Lane 1983; Xu and Terakawa 1999). In copepods, however, the source of the sheath remains uncertain. The cell type of those cell bodies occasionally found myelin-wrapped could not be determined. In general, the myelin of all copepods surveyed was conspicuous by its lack of association with cell bodies and glial cytoplasm. At the nodes, myelin laminae appear to have a close association with the nerve cell (Fig. 7E).

Nodes

Circumferential nodes completely encircling the axons (nodes of Ranvier), typical of vertebrate myelin, have also been described for the prawn (Heuser and Doggenweiler 1966). In copepods, the nodes shared features of “fenestration” nodes of penaeids (Hsu and Terakawa 1996) and “focal” nodes of earthworm (Günther 1976) in that only a portion of the circumference of the

Table 2 Comparison of myelin. Characteristics of the structure and physiology of myelin in vertebrates, copepods, decapods (palaemonids and penaeids) and annelids are compared. Sources for comparative information are: vertebrate, Ritchie (1984); copepod,

present study; penaeid, Hama (1966); Xu and Terakawa (1999); palaemonid, Holmes et al. (1942); Heuser and Doggenweiler (1966); and annelid, Günther (1976); Roots and Lane (1983)

Characteristic	Vertebrate	Copepod	Penaeid	Palaemonid	Annelid
Wrap	Spiral	Concentric	Concentric	Concentric	Spiral/concentric
Origin	Oligodendrocytes	?	Glia	Glia	Glia
	Schwann cells				
Location	CNS and peripheral	CNS and peripheral	CNS	CNS	CNS, giant fibers
Seams	No	No	Aligned	Anti-aligned (alternating)	No
Attachment zones	No	No	Yes	Yes	Yes
Leaflet fusion	Cytoplasmic	Cytoplasmic	Cytoplasmic	Extracellular	Extracellular
	Extracellular	Extra-cytoplasmic			
Glial nuclei	External	?	Internal	Internal	Internal
Nodes	Circumferential	Focal	Focal (fenestration)	Circumferential	Focal
Periaxonal space	Small	Small	Large cellular	Small	Small
Max. cond. velocity	100 m s ⁻¹		200 m s ⁻¹	23 m s ⁻¹	30 m s ⁻¹

axolemma was exposed to extracellular space surrounding the nerve fiber. The association of copepod myelin lamellae with the axolemma or a closely associated density appears to present a somewhat different picture from that of other nodes. Neither paranodal cytoplasmic loops and analogous structures found in vertebrates, annelids, and prawns (Roots 1984), nor the interdigitated axonal and glial-cell membranes found in penaeids (Hsu and Terakawa 1996) were apparent. The functional ramifications of these morphological features are discussed below.

Myelin electrical structure

Myelin sheaths derive their function from two electrical properties: they serve to electrically insulate the nerve fiber (Ranvier 1878), decreasing transverse "leakage" conductance between the axon core and the outside of the fiber, and they decrease transverse capacitance that shunts rapidly changing currents. This reduces the ionic currents needed for the propagation of nerve impulses (and hence metabolic costs). It increases the length constant of the fiber, allowing axial current to spread to distant nodes. The restricted surface area of the node decreases the time the current requires to charge it so that it is rapidly activated. The combination produces the increase in propagation velocity. To achieve these electrical properties, the insulating (high resistance) properties of the myelin membrane must not be compromised by shunts. One point of potential compromise is at a node, where the necessity of terminating the myelin sheath introduces a possibility for current generated by nodal membrane to leak between the layers of myelin or between the myelin and the internodal axolemma. This would open shunts that would increase current requirements and enhance the amount of membrane needing to be charged, hence also slowing nodal depolarization and decreasing length constants. Myelin of earthworms and prawns possess structures in the paranodal region that appear to restrict leakage of current (Heuser and Doggenweiler 1966; Roots 1984). Vertebrate paranodal terminations of the myelin sheath are via close apposition of sheath membrane and axolemma along with membrane specializations and proteins, which likely have a similar function (Robertson 1959; Rosenbluth 1984; Bellen et al. 1998). Copepods appear to lack desmosome-like specializations in the paranodal region. Instead, myelin membrane becomes intimately associated with the axolemma, if not fused with it. This close association may serve the function of restricting current leakage.

A second consideration is radial escape of current through the internode. A spirally wrapped sheath, or a concentrically-layered one interrupted by seams, is inherently inefficient at reducing such leakage compared with concentrically arranged seamless laminae. Provisions must be made to prevent current from passing along the cytoplasm or external surface of a layer or

through a seam. Increasing the number of wraps and decreasing or occluding the space between laminae are two ways to reduce leakage in such cases. In vertebrates, such leakage is avoided by the fusion or near fusion of both intracellular and extracellular leaflets of the myelin, leading to a generally more compact myelin than is typical of invertebrates. In the myelinated calanoids such measures are not needed in seamless concentric myelin.

Acknowledgements We thank M. Aeder, M.R. Andres and K.K. Wong for participation in the copepod collections, P. Hassett, A. Kitalong and J. Yen for assistance in collecting and identifying copepods, R. Young for providing us with copepods, F. Ferrari for assistance with the taxonomic terminology, and L. Bartram for participation in setal counts and analysis. The Hawaii Institute of Marine Biology and Friday Harbor Laboratories kindly allowed us to use their facilities and boats for copepod collections. The Natural Energy Laboratory of Hawaii provided access to the deep-water pipes at Ke'ahole Point, Hawaii. The research was supported by NSF grants OCE 89-18019 and OCE 95-21375 and NIH grant RR03061. Experiments complied with the "Principles of animal care" publication No. 86-23 of the National Institutes of Health and with the current laws of the USA.

References

- Barrientos YC (1980) Ultrastructure of sensory units on the first antennae of calanoid copepods. M.S. Thesis, University of Ottawa, Ottawa, Ontario
- Bellen HJ, Lu Y, Beckstead R, Bhat MA (1998) Neurexin IV, caspr and paranodin – novel members of the neurexin family: encounters of axons and glia. *Trends Neurosci* 21: 444–449
- Boxshall GA (1985) The comparative anatomy of two copepods, a predatory calanoid and a particle-feeding mormonilloid. *Philos Trans R Soc Lond B* 311: 303–377
- Boxshall GA (1992) Copepoda. In: Harrison FW, Humes AG (eds) *Microscopic anatomy of invertebrates*, vol 9. Crustacea. Wiley-Liss, New York, pp 347–384
- Bullock TH, Horridge GA (1965) *Structure and function in the nervous system of invertebrates*, vol I. Freeman, San Francisco
- Bundy MH, Paffenhöfer GA (1993) Innervation of copepod antennules investigated using laser scanning confocal microscopy. *Mar Ecol Prog Ser* 102: 1–14
- Davis AD, Weatherby TM, Hartline DK, Lenz PH (1999) Myelin-like sheaths in copepod axons. *Nature (Lond)* 398: 571
- Fleminger A (1985) Dimorphism and possible sex change in copepods of the family Calanidae. *Mar Biol* 88: 273–294
- Friede RL, Samorajski T (1967) Relation between the number of myelin lamellae and axon circumference in fibers of vagus and sciatic nerves of mice. *J Comp Neurol* 130: 223–232
- Gill CW (1985) The response of a restrained copepod to tactile stimulation. *Mar Ecol Prog Ser* 21: 121–125
- Gill CW (1986) Suspected mechano- and chemosensory structures of *Temora longicornis* Müller (Copepoda: Calanoida). *Mar Biol* 93: 449–457
- Govind CK, Pearce J (1988) Remodeling of nerves during claw reversal in adult snapping shrimps. *J Comp Neurol* 268: 121–130
- Günther J (1976) Impulse conduction in the myelinated giant fibers of the earthworm. Structure and function of the dorsal nodes in the median giant fiber. *J Comp Neurol* 168: 505–532
- Hama K (1966) The fine structure of the Schwann cell sheath of the nerve fiber in the shrimp (*Penaeus japonicus*). *J Cell Biol* 31: 624–632
- Hartline DK, Lenz PH, Herren CM (1996) Physiological and behavioral studies of escape responses in calanoid copepods. *Mar Fresh Behav Physiol* 27: 199–212

- Heuser JE, Doggenweiler CF (1966) The fine structural organization of nerve fibers, sheaths, and glial cells in the prawn, *Palaemonetes vulgaris*. *J Cell Biol* 30: 381–403
- Holmes W, Pumphrey RJ, Young JZ (1941) The structure and conduction velocity of the medullated nerve fibres of prawns. *J Exp Biol* 18: 50–54
- Hsu K, Terakawa S (1996) Fenestration in the myelin sheath of nerve fibers of the shrimp: a novel node of excitation for saltatory conduction. *J Neurobiol* 30: 397–409
- Huys R, Boxshall GA (1991) Copepod evolution. Ray Society, Unwin Brothers, Old Woking
- Kusano K (1966) Electrical activity and structural correlates of giant nerve fibers in Kuruma shrimp (*Penaeus japonicus*). *J Cell Physiol* 68: 361–384
- Lenz PH, Weatherby TM, Weber W, Wong KK (1996) Sensory specialization along the first antenna of a calanoid copepod, *Pleuromamma xiphias* (Crustacea). *Mar Fresh Behav Physiol* 27: 213–221
- Lenz PH, Hartline DK, Davis AD, Weatherby TM (2000) The need for speed. I. Fast reactions and myelinated axons in copepods. *J Comp Physiol A* 186: 337–345
- Lowe E (1935) On the anatomy of a marine copepod, *Calanus finmarchicus* (Gunnerus). *Trans R Soc Edinburgh* 58: 560–603
- Moore JW, Joyner RW, Brill MH, Waxman SD, Najjar-Joa M (1978) Simulations of conduction in uniform myelinated fibers: relative sensitivity to changes in nodal and internodal parameters. *Biophys J* 21: 147–160
- Morell P (ed) (1984) Myelin, 2nd edn. Plenum Press, London
- Park TS (1966) The biology of a calanoid copepod *Epilabidocera amphitrites* McMurrich. *Cellule* 66: 129–251
- Ranvier L (1878) Leçons sur l'histologie du système nerveux. Libraire F. Savy, Paris
- Ritchie JM (1984) Physiological basis of conduction in myelinated nerve fibers. In: Morell P (ed) Myelin. Plenum Press, New York, pp 117–145
- Robertston JD (1959) Preliminary observations of the ultrastructure of nodes of Ranvier. *Z Zellforsch Mikrosk Anat* 50: 553–560
- Roots BI (1984) Evolutional aspects of the structure and function of the nodes of Ranvier. In: Zagoren JC, Fedoroff S (eds) The node of Ranvier. Academic Press, Orlando, pp 1–29
- Roots BI, Lane NJ (1983) Myelinating glia of earthworm giant axons: thermally induced intramembranous changes. *Tissue Cell* 15: 695–709
- Rosenbluth J (1984) Membrane specialization at the nodes of Ranvier and paranodal and juxtapanodal regions of myelinated central and peripheral nerve fibers. In: Zagoren JC, Fedoroff S (eds) The node of Ranvier. Academic Press, Orlando, pp 31–67
- Weatherby TM (1981) Ultrastructural study of the sinus gland of the crab, *Cardiosoma carnifex*. *Cell Tissue Res* 220: 293–312
- Weatherby TM, Wong KK, Lenz PH (1994) Fine structure of the distal sensory setae on the first antennae of *Pleuromamma xiphias* Giesbrecht (Copepoda). *J Crust Biol* 14: 670–685
- Xu K, Terakawa S (1999) Fenestration nodes and the wide submyelinic space form the basis for the unusually fast impulse conduction of shrimp myelinated axons. *J Exp Biol* 202: 1979–1989
- Zagoren JC, Fedoroff S (eds) (1984) The node of Ranvier. Academic Press, Orlando
- Yen J, Lenz PH, Gassie DV, Hartline DK (1992) Mechanoreception in marine copepods: electrophysiological studies on the first antennae. *J Plankton Res* 14: 495–512